Biochemistry and Biophysics Reports 40 (2024) 101868

Contents lists available at ScienceDirect

Biochemistry and Biophysics Reports

journal homepage: www.elsevier.com/locate/bbrep

Comprehensive characterization and metabolomics to explore the role of hydrocortisone-induced yin deficiency syndrome in mice

Wenqi Jin [a], Lan Yang [a], Yuxin Zhang [a], Yu Wang [b], Yingna Li [a], Yiming Zhao [a], Liwei Sun [a,c,*], Fangbing Liu [d,**]

[a] Research Center of Traditional Chinese Medicine, The Affiliated Hospital to Changchun University of Chinese Medicine, Changchun, China
[b] College of Traditional Chinese Medicine, Changchun University of Chinese Medicine, Changchun, China
[c] Key Laboratory of Active Substances and Biological Mechanisms of Ginseng Efficacy, Ministry of Education, Changchun, China
[d] Northeast Asian Institute of Traditional Chinese Medicine, Changchun University of Chinese Medicine, Changchun, China

ARTICLE INFO

Keywords:
Traditional Chinese medicine
Yin deficiency syndrome
Hydrocortisone
Metabolomics
Characterization

ABSTRACT

Yin deficiency syndrome is a theoretical concept of traditional Chinese medicine (TCM) that claims an imbalance between Yin and Yang serves as a potential etiological factor disrupting physiological homeostasis. Its diagnosis in TCM is hindered by the intricate and diverse etiology, resulting in the absence of quantification and standardization. Hence, this study developed a hydrocortisone (HC) induced Yin deficiency syndrome model to investigate the intricate network underlying TCM and elucidate its intervention mechanism. In the findings, the model was characterized by weight loss, elevated drinking water, yellow urination, dry stools, variations in inflammatory factors, and higher levels of oxidative stress. Based on metabolomics, 56 metabolites showed different expressions; among them, 19 were upregulated, and 37 were downregulated. Bioinformatics analysis revealed that identified metabolites are mainly involved in glycerol phospholipid metabolism, pyrimidine metabolism, amino acid biosynthesis, arginine and proline metabolism, and arachidonic acid metabolism pathways. Finally, the metabolic network association confirmed the diagnostic accuracy of the Yin deficiency syndrome as established by HC. We propose for the first time an animal model of Yin deficiency syndrome induced by hydrocortisone in TCM clinical state. This research presents experimental evidence for establishing TCM symptoms and serves as a fundamental basis for the scientific awareness of their etiology.

1. Introduction

Traditional Chinese medicine (TCM) theory for identifying and managing pathogenic causes and illnesses has persisted for over 2000 years. The cultural significance of TCM has recently attracted widespread international recognition. The human body maintains a relatively stable working state in terms of physiological function and mental state, which mainly depends on the balance of Yin and Yang. Dysregulation of Yin-Yang is widely recognized as a potential stimulus for pathological alterations and vulnerability to disease progression [1,2]. In Chinese medicine, Yin deficiency syndrome is not regarded as a disease, but a state of suboptimal health or an acute physiological stress response that can worsen health conditions [3]. This syndrome is characterized by internal heat (exuberant endogenous fire), which is presented by deterioration in physical functionality, weakness, emaciation, irritability, rapid weak or thready pulse, pale and red tongue, dryness of the oral cavity. Further progression may affect the craniofacial region's integumentary and mucosal structures, including erythema, edema, pyrexia, and discomfort. Individuals may experience xerophthalmia, polydipsia, oral ulcerations, gingival edema, and alterations in urinary coloration and bowel movements [4,5]. Emerging evidence indicates that the depletion of Yin may be attributed to various factors, including mental stress, environmental influences, living and dietary habits, etc [6]. With the development of the medical model centered on prediction, prevention and customization, it is particularly important to master the formation and prevention of Yin deficiency syndrome.

Yin deficiency syndrome is a physiological condition that results in dysregulation of the internal environment, influencing the neuroendocrine, metabolic, immune, and cardiovascular systems, etc. This

* Corresponding author. Research Center of Traditional Chinese Medicine, the Affiliated Hospital to Changchun University of Chinese Medicine, Changchun, China.
** Corresponding author. Northeast Asian Institute of Traditional Chinese Medicine, Changchun University of Chinese Medicine, Changchun, China.
E-mail addresses: sunnylilwei@163.com (L. Sun), liufb@ccucm.edu.cn (F. Liu).

https://doi.org/10.1016/j.bbrep.2024.101868
Received 12 October 2024; Received in revised form 1 November 2024; Accepted 7 November 2024

disturbance affects the biological system's delicate equilibrium between Yin and Yang. The fundamental investigation of TCM states that yin deficiency syndrome is strongly associated with the hyperactivity of the hypothalamic-pituitary-adrenal (HPA) axis, which causes the disruption of hormone secretion by target glands and a subsequent decrease in the coordination among various systems axis [7]. The HPA hyperactivity can lead to sympathetic hyperexcitability and elevated susceptibility to hyperthyroidism [8]. Besides, the increased serum cortisol/testosterone ratio may be one of the indicators of internal heat in Yin deficiency. Research findings suggest that cortisol and adrenocorticotropic hormone (ACTH) are elevated in the state of Yin deficiency [9], highlighting the involvement of the HPA axis [7]. The release of glucocorticoids (GCs) modulates mitochondrial calcium homeostasis and reactive oxygen species (ROS) generation, causing immunosuppression [10]. In addition, the long-term excessive secretion of GCs can lead to disorders of glucose and lipid metabolism and increase the susceptibility of the body to metabolic diseases. In terms of glucose metabolism, it can antagonize glucose homeostasis and insulin sensitivity, and can also prevent the absorption of glucose by renal tubules and increase blood glucose [11]. The elevated levels of circulating free fatty acids (FFA) and ketone bodies in lipid metabolism stimulate lipid peroxidation (LPO), leading to the worsening of cellular dysfunction [12]. Sustained circulating glucocorticoid levels trigger reduced nitric oxide (NO) bioavailability, leading to endothelial dysfunction, and transcription of pro-inflammatory factors further exacerbating deleterious outcomes [13]. Notably, the primary metabolic role of GCs is to enhance the accessibility of energy substrates. In support of this claim, research suggests that the internal heat in Yin deficiency substantially influences the body's energy metabolism [6,14]. Adverse consequences resulting from the metabolic alterations induced by GCs could potentially reveal specific symptoms linked to Yin deficiency.

Recently, significant progress has been made in understanding and improving Yin deficiency syndrome. However, there remains a lack of explicit characteristics or scientific proof to explore its biological mechanism fully. Previous investigations utilized thermogenic botanicals, such as *Zingiberis Rhizoma* (Ganjiang in Chinese), *Cortex Cinnamomi* (Rougui in Chinese), and *Aconiti Lateralis Radix Praeparata* (Fuzi in Chinese), *Dimocarpus longan* Lour (Longyan in Chinese), to elicit food-borne internal heat according to the theories of TCM [15,16]. Likewise, animal models that use GCs to induce a drug-induced endothermic state are available [17]. The purpose is to provide more insights for subsequent diagnosis and correction of this sub-health state. Due to the inherent subjectivity of TCM diagnosis, systems biology provides a promising approach to investigating the intricate mechanisms behind TCM syndromes. Systems biology quantitatively collects comprehensive data on multidirectional physiological changes in order to reveal the overall functional state of the human body. In this investigation, we used hydrocortisone (HC), a GC, induced Yin deficiency syndrome in mice to observe and analyze the alterations in basic physiological signs, organ morphology, and cytokine levels in *vivo*. The Metabolomics approach was applied to investigate the serum of mice exhibiting Yin deficiency syndrome. Bioinformatics analysis complemented this approach to determine the functional metabolic aspects of HC-induced Yin deficiency syndrome. This research elucidated the scientific foundations and biological mechanisms underlying the basic concepts of TCM. It offered valuable insights that can effectively direct the advancement of modern TCM precision therapies and promote overall well-being.

2. Materials and methods

2.1. Reagents

Hydrocortisone (HC) was purchased from Sigma-Aldrich (St. Louis, MO, USA). Enzyme-linked immunosorbent assay (ELISA) kits for tumor necrosis factor-α (TNF-α), interleukin 6 (IL-6), interleukin 10 (IL-10) and monocyte chemotactic protein-1 (MCP-1) were purchased from IBL International GmbH, Hamburg, Germany). Biochemical activity assay kits for total antioxidant capacity (T-AOC), superoxide dismutase (SOD), catalase (CAT) and malondialdehyde (MDA) were purchased from Nanjing Jiancheng Institute of Biotechnology. All utilized reagents were analytical grade and purchased from Fisher Scientific (Fair Lawn, NJ, USA).

2.2. Animal and model design

Experimental animals comprised 8 weeks old C57BL/6 male mice, obtained from Changchun Gaoxin Medicine Animal Experimentation Center (Jilin, China). The mice were maintained in a standard environment with a consistent temperature (23 ± 2 °C) and humidity (60 ± 5 %) with a light/dark cycle of 12 h/12 h for 1 week. During the experimental duration, the animals were provided ad libitum access to food and water. Different doses of HC were used to detect the effect of simulating Yin deficiency syndrome in mice, based on which the model drug dose was determined and used for metabolomics detection. Animals were divided into the control and the model group. Mice were orally with HC (10, 20, 50 mg/kg) and every other day for 12 days. The saline (same volume) was similarly gavaged in the control group. All mice were monitored daily, and their body weights were noted upon continuous administration. After completion of the experiment, mice were euthanized, and blood was collected through cardiac puncture. Blood and tissue samples, including the spleen, adrenal glands, and thymus, were also harvested and weighed promptly. Organ index was calculated according to the following formula: organ index (mg/g) = organ weight (mg)/animal body weight (g). All animal experimental procedures are comply with ARRIVE (Animal Research: Report of in Vivo Experiments) guidelines and approved by the Animal Ethics Committee of Changchun University of Chinese Medicine (No. 2021483).

2.3. Quantification of antioxidant enzyme activity and inflammatory factors

Collected serum samples were thawed at 4 °C to examine the effects of inflammatory mediators and oxidative stress-related enzyme activity on HC-induced Yin deficiency syndrome. In accordance with the defined protocol for each kit, MDA was measured by TBA method, SOD by hydroxylamine method, T-AOC by ABTS method, and CAT by ammonium molybdate method. The incubation of serum takes place within microtiter wells with required dilution. Inflammatory mediators TNF-α, IL-6, IL-10 and MCP-1 were quantified by ELISA method. The procedure was performed corresponding to the instructions provided by the manufacturer.

2.4. Histopathological analysis

All harvested tissues were fixed with 4 % paraformaldehyde solution, followed by dehydration and embedding in paraffin. Subsequently, the embedded tissues were sectioned into 4 μm thickness. The slices were examined with Hematoxylin-eosin (H&E) staining followed by dewaxing, rehydration, and antigen retrieval. Observation was performed using an optical microscope.

2.5. Sample collection and processing

Blood was collected from each mouse using vacuum blood collection tubes without any additives. The serum was separated by allowing the sample to stand at ambient temperature for 2 h, after centrifugation at 3000 r/min for 10 min. The samples were frozen and preserved at −80 °C before subsequent examinations. The samples were thawed at 4 °C and 400 μL of a chilled solution (methanol/acetonitrile/water) (2:2:1, v/v) was introduced. The sample was vortexed, and incubated at −20 °C for 10 min after centrifuged. The resulting supernatant was dried

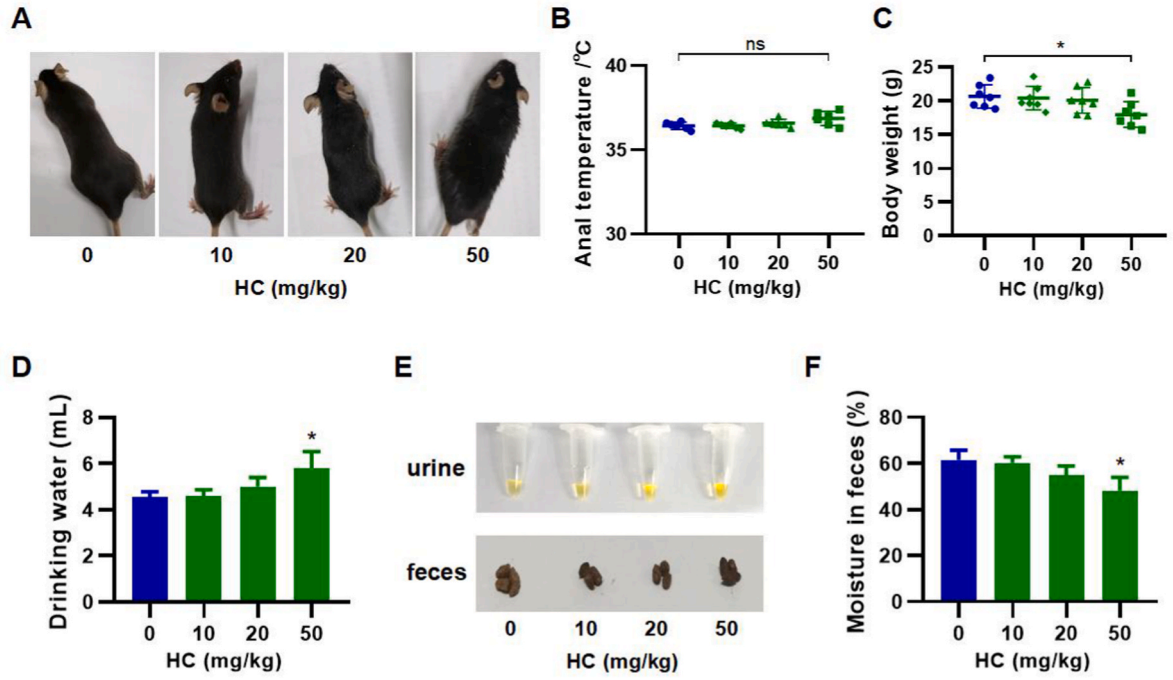

Fig. 1. The general signs of mice in the physiological saline (control) group and varying doses of HC (model) group were treated. (A) Hair gloss. (B) Anal temperature. (C) Body weight. (D) Water intake. (E) Excrement observation. (F) Moisture content of feces. Each value indicates the mean ± SD; $*p < 0.05$ and $**p < 0.01$.

in a vacuum. To perform mass spectrometry analysis, 100 μL of an acetonitrile aqueous solution (with water = 1:1, v/v) was utilized for reconstitution. The resulting mixture was centrifuged for 15 min at 14,000 g (4 °C). The collected supernatant was used for subsequent injection following centrifugation. To assess the stability of the system and the reliability of the collected data, equivalent amounts of samples were mixed to generate quality control (QC) samples. These samples were processed by using the same experimental procedure.

2.6. Metabolic profiling analysis of serum

The samples were examined using a liquid chromatography platform (1290 Infinity LC, Agilent Technologies) coupled with a Triple TOF 6600 system (AB SCIEX, CA, USA). Approximately 2 μL of the sample solution was introduced into a HILIC column (2.1 mm × 100 mm, ACQUITY UPLC BEH 1.7 μm, Waters) using a flow rate of 0.5 mL/min at 25 °C. The mobile phase contains a solution (25 mM ammonium acetate and ammonium hydroxide in water) (mobile phase A) and acetonitrile (mobile phase B). The gradient elution conditions employed for the analysis of serum samples were outlined below: 0–0.5 min, 95 % B; 0.5–7 min, 95%–65 % B; 7–8 min, 65%–40 % B, 8–9 min, 40 % B, 9–9.1 min, 40%–95 % B, 9.1–12 min, 95 % B. Electrospray ionization (ESI) source parameters were determined to HILIC separation: Ion Source Gas1 (Gas1) and Ion Source Gas2 (Gas2) were both 60, Curtain gas (CUR) was 30, source temperature (ST) was 600 °C. IonSapary Voltage Floating (ISVF) was adjusted to ± 5500 V, depending on the positive or negative ion mode. The secondary mass spectra of product ions were acquired by applying information-dependent acquisition (IDA) with the high-sensitivity mode selected. The range of the scan was between *m/z* 25–1000 Da. The following parameters were set: the collision energy (CE) was 35 ± 15 eV; the declustering potential (DP) was ±60 V; excluding isotopes within 4 Da, there were 10 candidate ions per cycle to monitor.

2.7. Data processing

Raw data was processed via ProteoWizard to convert it into the mzXML format. The raw data undergo a series of preprocessing steps using the XCMS software package in the R programming language. These steps included baseline filtration, peak identification, integration, retention time correction, and peak alignment. Univariate analysis, using volcano plots, was utilized to detect the metabolite expressions within the dataset in response to the experimental factors. The volcano plots were generated based on fold change values (FC > 1.5 or FC < 0.67) and corresponding p-values. SIMCA-P software (version 14.1, Umetrics AB, Umea, Sweden) was used to import data matrix for multivariate statistical analysis, specifically principal component analysis (PCA) and orthogonal partial least-squares discriminant analysis (OPLS-DA). Meanwhile, the value of variable importance projection (VIP) was quantified for the OPLS-DA model projection to reflect the extent of its contribution towards the classification. The quality of the models was assessed using a 7-fold cross-validation approach, evaluating R^2Y (model to class variability Y) and Q^2 (model predictability) metrics. The proximity to "1" indicates a higher level of stability and reliability exhibited by the model. The significance of each metabolite was assessed using the rate-corrected *t*-test, and the resulting p-value was determined. The biomarker candidates were recognized as the differential metabolites that met the criterion of VIP >1.0 and a p-value of <0.05. The identification and confirmation of metabolic differences were based on the mass-to-charge ratio (*m/z*) information obtained from the publicly available databases, HMDB and KEGG. The network analysis was executed to examine the correlation between endogenous metabolites in the Yin deficiency state induced by HC. The reference database of KEGG was utilized to plot the correlation analysis network. This network was generated to elucidate and visually represent the impacted metabolic pathways.

2.8. Statistical analysis

The presented data were represented as means ± standard deviation and obtained from three different experiments. One-way analysis of variance (ANOVA) was applied to examine the significance of differences between groups using GraphPad Prism 8.0 (San Diego, CA, USA). The significance value $p < 0.05$ was deemed statistically significant.

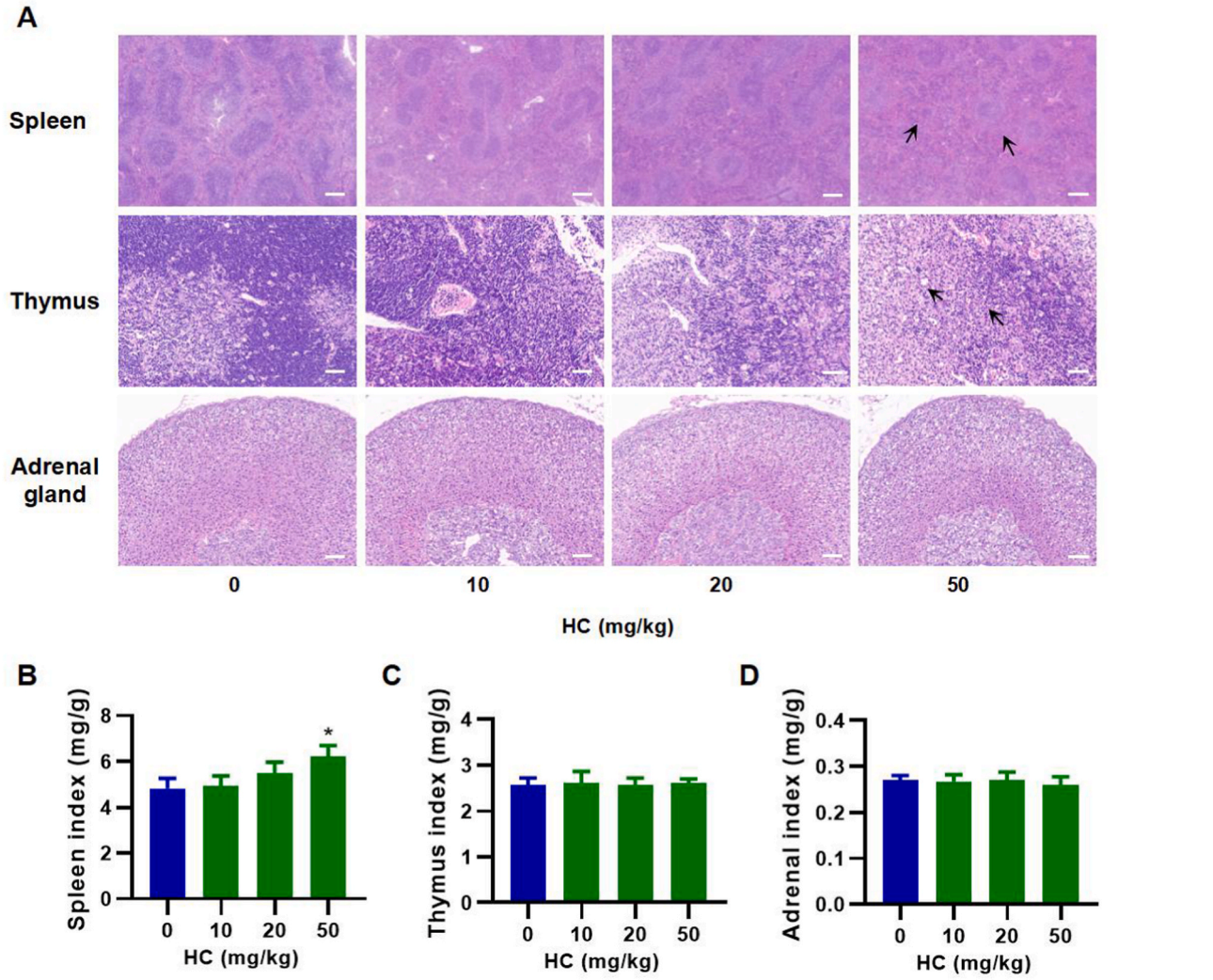

Fig. 2. Histological examinations and organ indices in HC-induced Yin deficiency syndrome. (A) Histopathological staining of the spleen, thymus and adrenal gland tissue. (B–D) Spleen, thymus and adrenal gland indices. Scale bar = 50 μm. Each value indicates the mean ± SD; $*p < 0.05$.

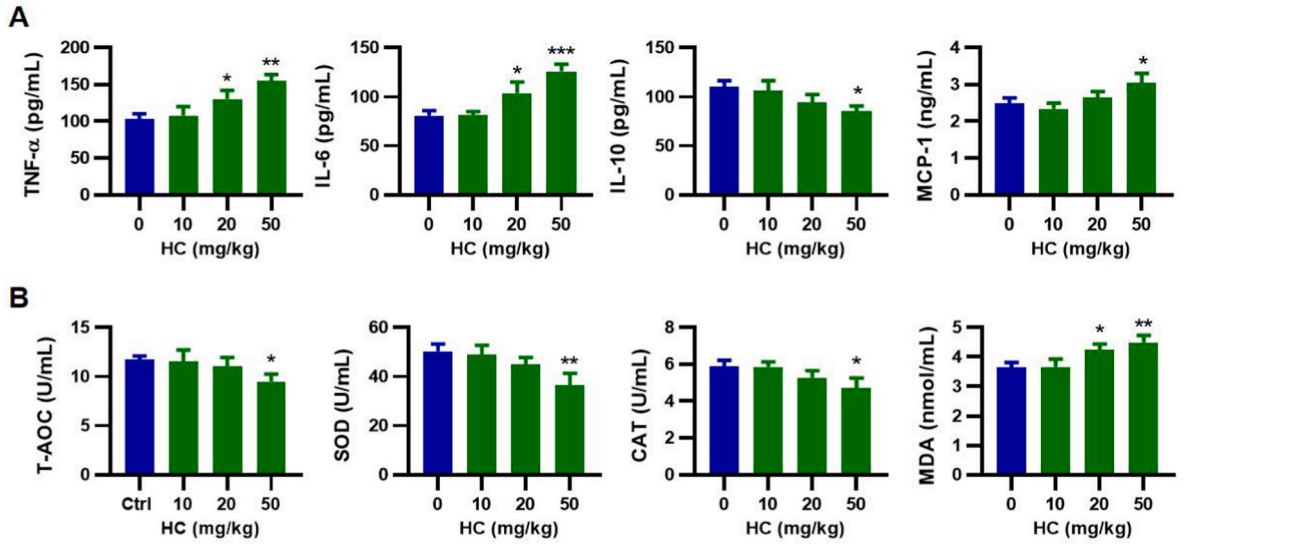

Fig. 3. The changes in inflammatory factors and oxidative stress indicators administered to HC in mice. (A) Serum concentration of inflammatory mediator, TNF-α, IL-6, IL-10 and MCP-1 in mice. (B) Serum antioxidant enzyme activities of T-AOC, SOD, CAT and MDA in mice. Each value indicates the mean ± SD; $*p < 0.05$ and $**p < 0.01$.

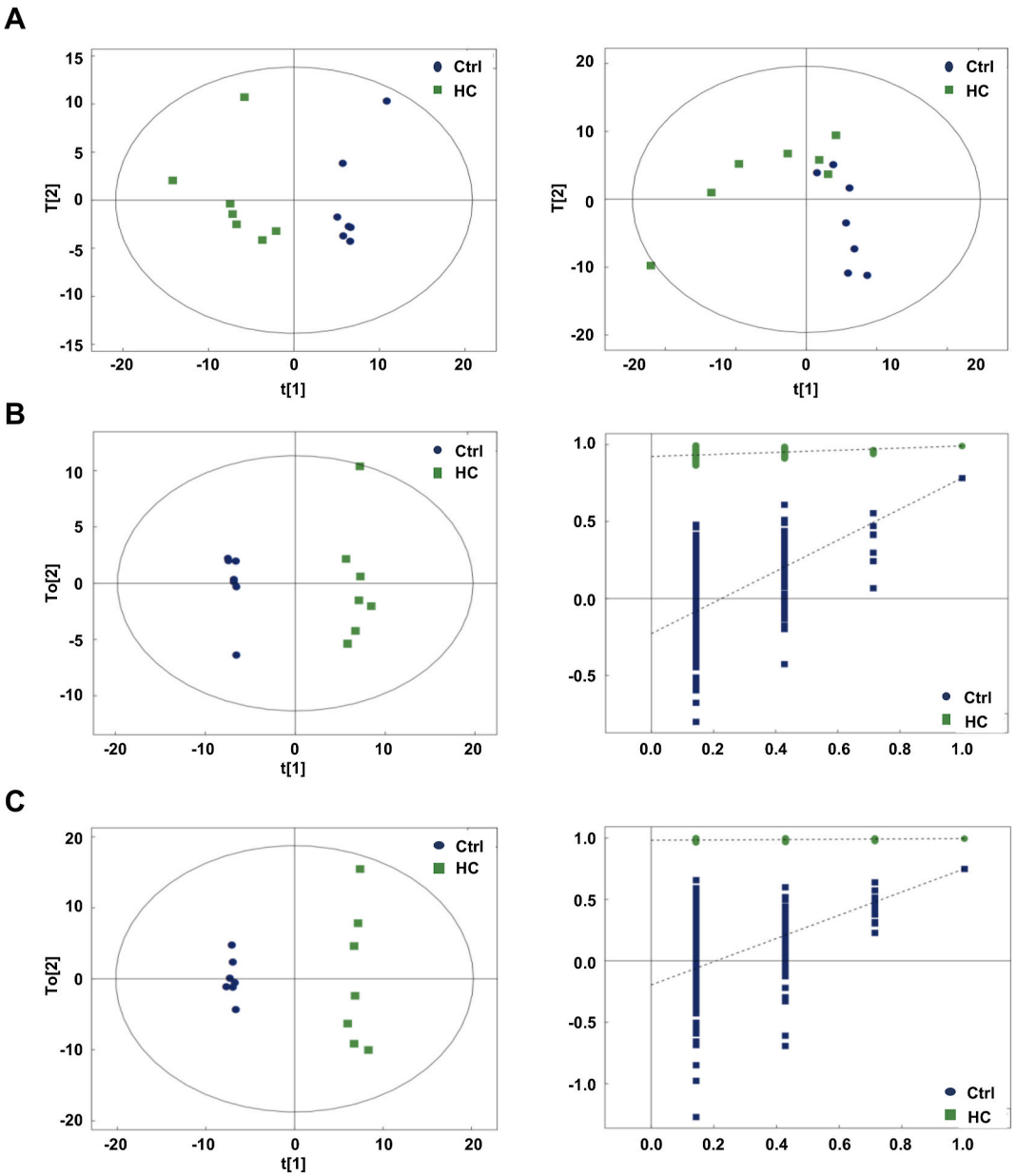

Fig. 4. Metabolic profiling-based multivariate statistical analysis. (A) PCA score plot from the control group and HC (50 mg/kg)-induced Yin deficiency syndrome group. (B) OPLS-DA model derived from dispersion point map and the result of the permutation test in a positive ion mode. (C) OPLS-DA model generated the dispersion point map and the result of the permutation test in a negative ion mode.

3. Results

3.1. Assessment of hydrocortisone on yin deficiency model in mice

3.1.1. Behavioral analysis and basic biological characterization of mice

Investigating Yin deficiency syndrome in mice through changes in their overall behavioral patterns. Mice in the HC drug-induced model group displayed hyperactivity and irritability following HC induction, along with weight loss, thinned fur, yellow urine, and dry stools. (Fig. 1A). Anal temperature, as a sign of internal heat, was found to be slightly elevated in the HC drug group, but not statistically significant (Fig. 1B). This is also in line with the Yin deficiency of the body feel heat, rather than fever. Body weights loss and water intake of the mice model were substantially increased of the control mice group at the end of the experiment (Fig. 1C and D). Moreover, the concentration of pigment was higher in the urine of model mice, while the moisture content of their feces decreased significantly (Fig. 1E and F). These symptoms corresponded with the Chinese medical description of Yin deficiency syndrome.

3.1.2. The effect of hydrocortisone on different organ of mice

Based on the tissue changes in the immune and endocrine organs of mice, the potential effects of the basic theories of traditional Chinese medicine have been demonstrated. In the HC drug group, the demarcation between both pulps (red and white) of the spleen exhibited a blurred appearance, with a less dense arrangement and decreased lymphocytes, in contrast to the typical morphology in the control group (Fig. 2A). Meanwhile, the coefficient of the spleen exhibited a substantial increase in the model (Fig. 2B). The cells within the lymphoid region of the thymus in mice treated with HC exhibits a loose arrangement characterized by irregularly shaped cells that undergo nuclear pyknosis, as indicated by the arrow. The histological examination of the adrenal gland revealed distinct demarcation of the cortical regions, including the zona glomerulosa and zona fasciculata, as well as the medullary regions,

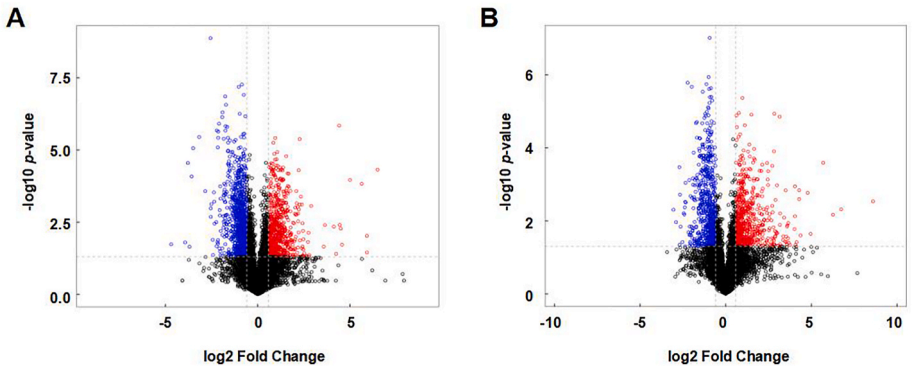

Fig. 5. Volcanic map of the differential metabolites in the positive (A) and negative (B) ion modes for the control and the model groups. Substantially upregulated metabolites were represented in red, decreased metabolites in blue, and insufficient differential metabolites were represented in black. (For interpretation of the references to color in this figure legend, the reader is referred to the Web version of this article.)

in both experimental groups. In contrast to the control, the model group revealed a slight reduction in the quantity of unit cells within the outer layer of the fascicular zone. However, no significant degeneration was observed (Fig. 2A). Besides, there was no statistically significant distinction in the indices of the thymus and adrenal tissues (Fig. 2C and D). These outcomes elucidate that the clinical symptoms of HC-induced immune system and metabolic disorders may be a potential mechanism of Yin deficiency syndrome.

3.1.3. The effect of hydrocortisone on inflammation and oxidative indicators in mice

To assess the effect of HC drug on internal environment disorder, the changes in inflammation and oxidative stress factors were measured before and after the HC intervention. On the 7th day of HC administration, the expressions of TNF-α, IL-6, and MCP-1 were considerably upregulated, while the levels of IL-10 were substantially decreased (Fig. 3A). After HC intervention, the activities of T-AOC, SOD, and CAT were remarkably reduced in contrast to the control group, while the levels of MDA exhibited an upward trend (Fig. 3B). The findings align with the description of a decrease in nonspecific resistance and suboptimal health in Yin deficiency syndrome. Based on the above results, we confirmed that a mouse model of Yin deficiency syndrome model was successfully constructed at a HC dose of 50 mg/kg.

3.2. Metabonomics and bioinformatics analysis

3.2.1. Effects of hydrocortisone on metabolic profiles

Initial observation was made regarding identifying 910 characteristics in the positive ion (+ve) mode, while 511 distinct characteristics in the negative (-ve) ion mode, in serum samples using UHPLC-Q-TOF MS. The total ion chromatograms (TIC) of QC samples exhibited a high overlap, indicating a consistent and uniform distribution of ions across the samples. Subsequently, unsupervised PCA and supervised OPLS-DA were analyzed to elucidate the comprehensive alterations in the metabolome of the Yin deficiency model. As evidenced by the PCA score plots (Fig. 4A and B), serum samples from both modes failed to show any apparent outliers. Notably, an automatic distinct separation was noted in the (+ve) mode, but not observed in the (-ve) mode. The OPLS-DA models were used to examine the distinguishability between the HC and Ctrl samples in (+ve) and (-ve) ion modes. The results indicate that the model was not overfitted ($R^2Y = 0.979$, $Q^2 = 0.361$ in positive ion mode; $R^2Y = 0.998$, $Q^2 = 0.292$ in negative ion mode), suggesting a satisfactory predictive performance (Fig. 4C). Additionally, this indicated that more accurate inter-metabolite group divisions and related facts were captured.

3.2.2. Identification of serum differential metabolites by hydrocortisone intervention

The visual identification of the metabolic global profiles of the differential metabolites was conducted via volcano plots. In the volcano plot, metabolites exhibiting low differences in fold change between the two samples are observed near the central region. Conversely, metabolites displaying substantial upregulation (FC > 1.5) are depicted as red plots, whereas metabolites exhibiting significant downregulation (FC < 0.67) are indicated as blue plots (Fig. 5A and B). In the subsequent analysis, differential metabolites were identified using secondary mass spectral matching ($p < 0.05$ and VIP >1). Approximately 56 metabolites with different expressions were detected, with an increased level of 19 metabolites and a decreased level of 37 metabolites in the HC model in contrast to the control (Table 1).

3.2.3. Evaluation of metabolic enrichment and pathway in yin deficiency state

Pathway enrichment and topological analyses were subsequently conducted on the differential metabolites. As observed in Fig. 6, the expression of HC-induced Yin deficiency state primarily corresponds to various biochemical processes that include metabolic pathways of glycerophospholipid, pyrimidine, phenylalanine, as well as biosynthesis of phenylalanine, tyrosine, and tryptophan.

3.2.4. Analysis of target and metabolic network in yin deficiency state

The identified metabolites in the above analysis exhibit functional similarities or complementarity and are involved in diverse metabolic processes within the human body via positive or negative regulation. The visualization of the interactions among distinct metabolites was depicted using the metabolic network (Fig. 7). In the stage of Yin deficiency, a notable downregulation was noted in the metabolic pathways of glycerophospholipids, pyrimidines, and amino acid biosynthesis. Conversely, arachidonic acid metabolism exhibited an upregulation, resulting in a disruption of metabolic processes. This imbalance in metabolism is indicative of a complex Yin deficiency syndrome.

4. Discussion

Yin deficiency is a multifaceted response characterized by a lack of specific physiological markers, in which the body's equilibrium is disrupted due to genetic factors or living habits such as exhaustion of the body liquid [18]. Previous investigations have documented that individuals exhibiting Yin deficiency syndrome display compromised immune function, disrupted lipid/protein metabolism, heightened irritability, and reduced adaptability, negatively impacting both quality of life and productivity [19,20]. Still, the biological properties and mode of action have not been fully studied and understood. In the current investigation, a high dosage of HC was administered to induce a state of

Table 1
Comparison of differential endogenous metabolites of mice in the HC-induced model and control group.

No.	Metabolites	rt(s)	*m/z*	Ion mode	Changing trend	VIP	*p*-Value	HMDB ID
1	Glutathione	493.664	611.142	neg	↓	1.659	3.65E-04	3337
2	*cis*-Aconitate	443.542	173.009	neg	↓	1.693	6.80E-03	72
3	Mesaconic acid	443.542	129.019	neg	↓	1.9	6.80E-03	749
4	Gossypol	406.541	501.196	pos	↑	1.666	2.84E-02	723
5	Amprenavir	405.564	528.195	pos	↑	1.173	4.14E-02	14,839
6	Trioxsalen	400.89	457.159	pos	↑	1.678	1.23E-02	15,575
7	dl-Glutamic acid	398.633	148.059	pos	↓	1.727	1.28E-03	60,475
8	Myo-inositol	391.535	179.056	neg	↑	4.604	3.10E-04	211
9	sn-Glycerol 3-phosphoethanolamine	389.101	214.048	neg	↓	3.514	1.57E-04	114
10	Asparagine	385.799	131.035	neg	↓	1.14	4.81E-02	168
11	Glycerophosphocholine	381.035	256.095	neg	↓	1.18	5.02E-06	86
12	Glycerol 3-phosphate	380.682	171.006	neg	↓	1.369	1.15E-06	126
13	Uric acid	380.661	167.044	neg	↑	3.601	2.03E-03	289
14	Phosphocholine	380.447	242.079	neg	↓	2.766	2.43E-06	1565
15	Sucrose	363.41	341.107	neg	↓	2.04	2.94E-02	258
16	Creatine	347.088	130.062	neg	↓	3.111	4.00E-04	64
17	5-aminosalicylic acid	343.918	136.047	pos	↓	4.033	5.43E-05	14,389
18	dl-tyrosine	319.52	182.08	pos	↓	1.134	2.15E-05	158
19	l-hydroxyarginine	318.664	116.07	pos	↓	5.143	2.36E-03	4224
20	1-methyladenosine	318.58	282.118	pos	↓	1.025	3.51E-02	3331
21	*N*-acetylhistidine	315.282	198.086	pos	↓	1.765	8.82E-03	14,748
22	4-Hydroxycinnamic acid	308.283	180.066	neg	↓	4.265	7.81E-04	2035
23	Trigonelline	289.129	138.055	pos	↓	4.698	4.80E-02	875
24	Caffeic acid	288.189	179.021	neg	↓	1.215	1.86E-05	3501
25	Glycerol 3-phosphate	281.857	152.996	neg	↓	1.755	1.01E-02	126
26	Phenylalanine	265.6	164.071	neg	↓	2.45	2.18E-02	159
27	Choline	263.323	104.107	pos	↓	18.589	2.14E-05	97
28	Cytidine	254.554	244.078	pos	↓	2.259	1.60E-04	89
29	b-hydroxybutyrate	238.563	103.04	neg	↑	2.266	3.20E-02	11
30	His-Lys	223.741	565.179	neg	↑	1.173	4.99E-02	133
31	Morphine-3-glucuronide	211.707	462.199	pos	↑	1.074	8.28E-04	41,936
32	7-methylguanine	194.591	166.071	pos	↓	1.9	3.04E-02	897
33	All-trans-4-hydroxyretinoic acid	190.825	315.195	neg	↑	4.897	4.71E-02	6254
34	1-Stearoyl-2-arachidonoyl-*sn*-glycerol	189.397	627.534	pos	↓	8.981	4.19E-03	7098
35	d-Glucuronolactone	181.594	175.025	neg	↑	2.317	2.00E-02	6355
36	l-dihydroorotate	181.482	157.037	neg	↓	6.984	3.62E-02	3349
37	*Trans*-traumatic acid	176.216	227.107	neg	↑	1.006	4.25E-04	933
38	Thromboxane b2	173.824	369.226	neg	↑	2.523	6.62E-04	3252
39	l-palmitoylcarnitine	165.078	400.341	pos	↑	7.272	6.42E-03	222
40	Deoxycholic acid	157.042	391.283	neg	↑	1.197	1.38E-02	626
41	*N*-(octadecanoyl)sphing-4-enine-1-phosphocholine	150.607	731.602	pos	↑	1.311	3.98E-03	1348
42	PC(16:0/16:0)	141.658	734.567	pos	↓	4.361	6.47E-04	564
43	Uracil	116.375	113.033	pos	↓	1.088	3.74E-03	300
44	Urea	104.406	61.039	pos	↓	3.67	2.31E003	294
45	Thymine	103.014	127.049	pos	↓	1.82	5.77E-03	262
46	His-ser	102.898	241.082	neg	↓	1.314	7.34E-03	273
47	3-hydroxyanthranilic acid	94.565	136.038	pos	↓	3.99	8.43E-03	1476
48	12s-hydroxy-5z,8e,10e-heptadecatrienoic acid	67.702	263.199	pos	↑	1.32	1.37E-04	12,535
49	Pyridine	65.708	80.049	pos	↓	1.641	2.86E-03	926
50	Niacinamide	65.093	123.055	pos	↓	10.327	4.72E-04	1406
51	Ricinoleic acid	57.31	297.242	neg	↑	1.615	9.13E-04	34,297
52	Linoleic acid	37.061	279.233	neg	↑	13.459	2.85E-03	673
53	Myristic acid	37.05	227.201	neg	↓	4.439	3.23E-03	806
54	Palmitic acid	37.05	255.233	neg	↑	5.85	3.46E-02	220
55	Oleic acid	36.985	303.232	neg	↓	6.514	1.66E-02	207
56	dl-normetanephrine	27.305	134.059	pos	↓	3.11	1.65E-02	819

Yin deficiency syndrome. Mice with phenotypic symptoms such as the appearance of yellow urine, dry stools, restlessness, increased water intake, and weight loss demonstrate an increased susceptibility to disease, thereby aligning with the clinical manifestations of patients with Yin deficiency syndrome. From the perspective of metabolomics, we found that the differentially expressed metabolites in the model mice were mainly concentrated in glycerophospholipid, amino acid, and pyrimidine metabolism, suggesting that variations in lipid metabolism, amino acid metabolism and energy metabolism could be attributed to the Yin deficiency state.

Phosphatidylcholine (PC, HMDB: 0000564) is a glycerophospholipid that is a predominant constituent within various cellular biofilms and is a primary source of lipid-based secondary messengers [21]. PCs comprise a polar head group containing phosphate, connected to the glycerol backbone, and two fatty acid residues. One of these fatty acid residues is saturated, while the other is unsaturated. The potential involvement of saturated PCs in regulating glucose homeostasis is suggested, as they may play an indirect role by serving as a substrate for diglyceride kinase delta. This particular enzyme is known to regulate glucose uptake in muscle cells. Unsaturated PCs are the primary target molecules for the peroxidation initiated by free radicals, such as ROS and RNS, generated by immune cells in response to inflammation and oxidative stress, which can damage cellular structures and functions [22]. The oxidation of PCs has been observed to potentially induce changes in lipid asymmetry, membrane turnover, and heightened membrane permeability [23]. Moreover, it functions as an endogenous ligand for the nuclear receptor PPARα and functions as a regulatory mediator in regulating gene expression related to lipid metabolism [24].

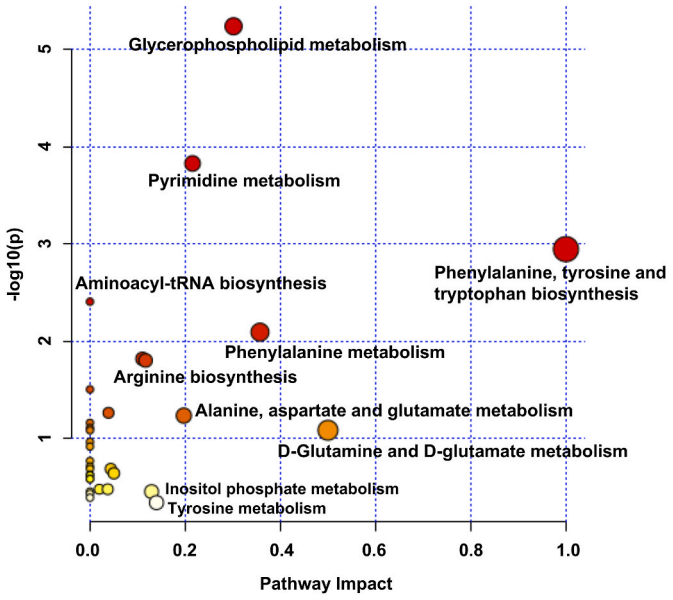

Fig. 6. Pathway analysis of HC-induced Yin deficiency syndrome mice. Each circle's dimensions and color were determined by the pathway impact and p values, respectively. The deeper the depth of the circle, the greater the metabolic pathway regulation by HC. The larger the circle, the increased endogenous metabolites in the metabolic pathway were regulated by HC. (For interpretation of the references to color in this figure legend, the reader is referred to the Web version of this article.)

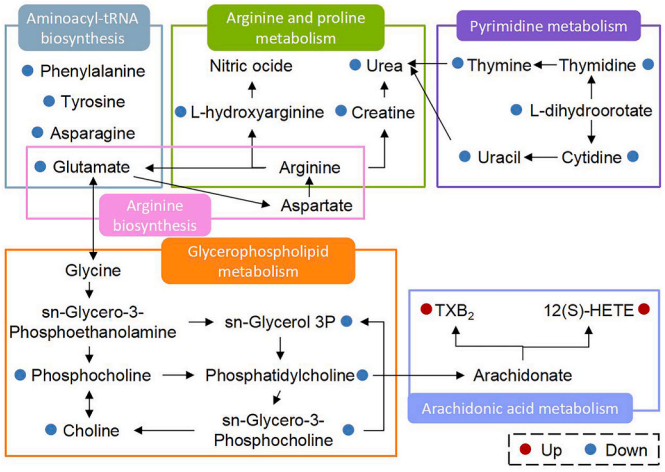

Fig. 7. Metabolic network of HC-induced Yin deficiency syndrome. The metabolites, which are marked in red dots, indicating up-regulation in the Yin deficiency syndrome group. The blue dots marked metabolite indicates down-regulation. (For interpretation of the references to color in this figure legend, the reader is referred to the Web version of this article.)

PPARα manipulate lipogenesis pathways and insulin signaling, thereby regulating fatty acid uptake, beta-oxidation and glycometabolism in muscles and liver [9]. In the model of HC-induced Yin deficiency, the downregulation of PCs may lead to the disturbance of cellular glycolipid metabolism, which in turn affects the body weight of mice. Choline (HMDB: 0000097), a vital nutrient and acetylcholine precursor, is essential in various physiological processes. The potential impact of lipid reduction on acetylcholine synthesis and availability is noteworthy, as it may contribute to metabolic changes with weight loss in mice exhibiting Yin deficiency.

Mitochondria are the primary pathways and mutual converting channels for amino acid metabolism. The origin of multiple carbon skeletons in the biosynthesis of amino acids can be traced back to the tricarboxylic acid (TCA) cycle [25]. It can undergo direct or indirect conversion into intermediates of the TCA cycle. Under the action of carboxylase in the body, phenylalanine generates tyrosine, aspartic acid generates glutamic acid through transamination, and the latter continues to transfer the amino group to oxaloacetic acid, generating α-Ketoglutaric acid and aspartic acid, or transferred to pyruvate [26,27]. The following aspartic acid, glutamic acid, phenylalanine, and tyrosine were downregulated in the serum metabolism profile of mice induced by HC, indicating that the amino acid metabolism in Yin deficiency syndrome mice was disrupted, indirectly leading to abnormal energy metabolism. The decomposition of arginine leads to urea and ornithine production via the catalytic activity of arginase, while the action of nitric oxide synthase (NOS) results in NO production [28]. The dysregulation of urea (HMDB: 0000294) and NO productions has been implicated in the modulation of renal osmotic pressure and the consequent impact on water metabolism in the body [29]. Meanwhile, the decrease in urea may be caused by insufficient protein intake, which is also a manifestation of loss of appetite in Yin deficiency syndrome. Creatine (HMDB: 0000064) is synthesized endogenously via the conversion of arginine in the liver, kidneys, and pancreas and is involved in facilitating cell energy supply and enhancing physical performance during exercise [30]. The findings of this study indicate that a decrease in creatine levels may align with the fatigue and weakness observed in individuals with Yin deficiency syndrome.

Arachidonic acid (HMDB: 0001043), classified as an essential amino acid, falls within the polyunsaturated long-chain amino acid group. Upon stimulation, it transforms into biologically active metabolites of eicosanoic acid via the catalytic activity of various metabolic enzymes, thereby regulating immune inflammation [31]. Thromboxane b2 (TXB2, HMDB: 0003252) involves many pathophysiological processes, such as platelet aggregation, atherosclerosis, and thrombosis. Its transformation is facilitated by the cyclooxygenase (COX), which acts as a channel [32]. The medium chain hydroxyeicosatetraenoic acid (HETE) concentration produced via the lipoxygenase (LOX) pathway substantially increases calcified blood vessels. Also, 12-HETE (HMDB: 0012,535) has a tendency to facilitate the upregulation of inflammatory mediators, consequently leading to a rise in vascular permeability [33]. It has been noted that 12-HETE is involved in the enhanced ROS production via activation of NF-κB, thereby regulating gene expression [34]. This research suggests a potential link between individuals exhibiting Yin deficiency and internal heat and the increased susceptibility to experiencing symptoms such as swelling and pain in the gums or local tissues. Oxidized lipids contribute to worsening oxidative stress, initiation of cell apoptosis, and an increased risk of various diseases with prolonged exposure. This study provides new ideas for the quantification and objectification of animal models of TCM syndromes.

5. Conclusion

This research introduces the first novel mouse model of Yin deficiency syndrome induced by HC in TCM state. Yin deficiency syndrome was assessed by extensively evaluating mouse biological characterization, physiological factor modifications, and differential metabolite changes. Most importantly, utilizing systems biology to reveal the interactions of multiple factors in the body was significantly based on the overall concept of TCM. While acknowledging the limitations of this study, it is necessary to emphasize the multi-factor testing in offering novel approaches to quantifying and objectifying TCM syndrome diagnosis. Thus, it is important to continue searching for comprehensive research and to elucidate biomarkers further to offer scientific elucidations for the intricate etiology and clinical mystery related to Yin deficiency syndrome.

CRediT authorship contribution statement

Wenqi Jin: Writing – original draft, Methodology, Investigation, Conceptualization. **Lan Yang:** Validation, Investigation, Data curation. **Yuxin Zhang:** Validation, Investigation, Formal analysis. **Yu Wang:** Methodology, Formal analysis. **Yingna Li:** Methodology, Formal analysis. **Yiming Zhao:** Methodology, Formal analysis. **Liwei Sun:** Supervision, Project administration, Conceptualization. **Fangbing Liu:** Supervision, Project administration, Conceptualization.

Data availability

Data will be made available on request.

Declaration of competing interest

The authors declare that they have no known competing financial interests or personal relationships that could have appeared to influence the work reported in this paper.

Acknowledgements

This work was supported by the Scientific and Technological Development program of Jilin Province (20230505033 ZP), the National Natural Science Foundation of China (U20A20402), the Synthetic Biotechnology Innovation Capacity Promotion Action Project of Tianjin (E1M0220101).

References

[1] Q. Hu, T. Yu, J. Li, Q. Yu, L. Zhu, Y. Gu, End-to-End syndrome differentiation of Yin deficiency and Yang deficiency in traditional Chinese medicine, Comput. Methods Progr. Biomed. 174 (2019) 9–15, https://doi.org/10.1016/j.cmpb.2018.10.011.
[2] Q. Yan, Stress and systemic inflammation: yin-yang dynamics in health and diseases, Methods Mol. Biol. 1781 (2018) 3–20, https://doi.org/10.1007/978-1-4939-7828-1_1.
[3] G. Liu, R. An, Applying a yin-yang perspective to the theory of paradox: a review of Chinese management, Psychol. Res. Behav. Manag. 14 (2021) 1591–1601, https://doi.org/10.2147/PRBM.S330489.
[4] T.T. Jiang, J.C. Li, Review on the systems biology research of Yin-deficiency-heat syndrome in traditional Chinese medicine, Anat. Rec. (2020), https://doi.org/10.1002/ar.24354.
[5] Y.J. Park, S.W. Cho, B.H. Lee, Y.B. Park, Development and validation of the Yin deficiency scale, J. Alternative Compl. Med. 19 (2013) 50–56, https://doi.org/10.1089/acm.2011.0677.
[6] T. Zhao, Z. Yang, X. Mei, L. Xu, Y. Fan, Metabolic disturbance in Korean red ginseng-induced "Shanghuo" (excessive heat), J. Ethnopharmacol. 253 (2020) 112604, https://doi.org/10.1016/j.jep.2020.112604.
[7] M.H. Pan, S.R. Zhu, W.J. Duan, X.H. Ma, X. Luo, B. Liu, H. Kurihara, Y.F. Li, J. X. Chen, R.R. He, "Shanghuo" increases disease susceptibility: modern significance of an old TCM theory, J. Ethnopharmacol. 250 (2020) 112491, https://doi.org/10.1016/j.jep.2019.112491.
[8] E. Nikolopoulou, D. Mytilinaios, A.E. Calogero, T.C. Kamilaris, T. Troupis, G. P. Chrousos, E.O. Johnson, Modulation of central glucocorticoid receptors in short- and long-term experimental hyperthyroidism, Endocrine 49 (2015) 828–841, https://doi.org/10.1007/s12020-015-0528-7.
[9] L. Wang, X. Zhao, J. Chen, X. Guo, X. Liang, D. Yi, H. Cui, Y. Liu, Biological indicators of sub-optimal health status, J. Tradit. Chin. Med. 33 (2013) 647–650, https://doi.org/10.1016/s0254-6272(14)60036-4.
[10] E. Kasahara, M. Inoue, Cross-talk between HPA-axis-increased glucocorticoids and mitochondrial stress determines immune responses and clinical manifestations of patients with sepsis, Redox Rep. 20 (2015) 1–10, https://doi.org/10.1179/1351000214Y.0000000107.
[11] Y. Lin, Z. Zhang, S. Wang, J. Cai, J. Guo, Hypothalamus-pituitary-adrenal Axis in Glucolipid metabolic disorders, Rev. Endocr. Metab. Disord. 21 (2020) 421–429, https://doi.org/10.1007/s11154-020-09586-1.
[12] K. Sikder, S.K. Shukla, N. Patel, H. Singh, K. Rafiq, High fat diet upregulates fatty acid oxidation and ketogenesis via intervention of PPAR-gamma, Cell. Physiol. Biochem. 48 (2018) 1317–1331, https://doi.org/10.1159/000492091.
[13] A.D. Kane, E.A. Herrera, Y. Niu, E.J. Camm, B.J. Allison, D. Tijsseling, C. Lusby, J. B. Derks, K.L. Brain, I.M. Bronckers, C.M. Cross, L. Berends, D.A. Giussani, Combined statin and glucocorticoid therapy for the safer treatment of preterm birth, Hypertension 80 (2023) 837–851, https://doi.org/10.1161/HYPERTENSIONAHA.122.19647.
[14] K. Luo, H. Zhao, B. Bian, X. Wei, N. Si, A. Brantner, X. Fan, X. Gu, Y. Zhou, H. Wang, Huanglian jiedu decoction in the treatment of the traditional Chinese medicine syndrome "Shanghuo"-An intervention study, Front. Pharmacol. 12 (2021) 616318, https://doi.org/10.3389/fphar.2021.616318.
[15] B. Li, X. Tao, L. Sheng, Y. Li, N. Zheng, H. Li, Divergent impacts on the gut microbiome and host metabolism induced by traditional Chinese Medicine with Cold or Hot properties in mice, Chin. Med. 17 (2022) 144, https://doi.org/10.1186/s13020-022-00697-2.
[16] N. Zhou, Y. Yang, K. Li, Y. Ke, X. Zheng, W. Feng, Z. Bai, T. Liu, Y. Wang, Z. Liu, X. Li, Integrating strategies of chemistry, biochemistry and metabolomics for characterization of the medication principle of "treating cold/heat syndrome with hot/cold herbs", J. Ethnopharmacol. 239 (2019) 111899, https://doi.org/10.1016/j.jep.2019.111899.
[17] R. Jin, B. Zhang, S.M. Liu, L. Ni, M. Li, L.Z. Li, [Mathematical analysis of characteristics of glucocorticoid-induced yang deficiency or yin deficiency syndrome in animal models based on information entropy theory], Zhong Xi Yi Jie He Xue Bao 9 (2011) 15–21, https://doi.org/10.3736/jcim20110104.
[18] L. Gan, T.T. Jiang, W.J. Yi, R. Lu, F.Y. Xu, C.M. Liu, Z.B. Li, Y.S. Han, Y.T. Hu, J. Chen, H.H. Tu, H. Huang, J.C. Li, Study on potential biomarkers of energy metabolism-related to early-stage Yin-deficiency-heat syndrome based on metabolomics and transcriptomics, Anat. Rec. 303 (2020) 2109–2120, https://doi.org/10.1002/ar.24355.
[19] C.M. Liu, J. Chen, S. Yang, L.G. Mao, T.T. Jiang, H.H. Tu, Z.L. Chen, Y.T. Hu, L. Gan, Z.J. Li, J.C. Li, The Chinese herbal formula Zhibai Dihuang Granule treat Yin-deficiency-heat syndrome rats by regulating the immune responses, J. Ethnopharmacol. 225 (2018) 271–278, https://doi.org/10.1016/j.jep.2018.05.001.
[20] C. Zhang, C.W. Tam, G. Tang, Y. Chen, N. Wang, Y. Feng, Spatial transcriptomic analysis using R-based computational machine learning reveals the genetic profile of yang or yin deficiency syndrome in Chinese medicine theory, Evid. Based Complement. Alternat. Med. 2022 (2022) 5503181, https://doi.org/10.1155/2022/5503181.
[21] N.D. Ridgway, The role of phosphatidylcholine and choline metabolites to cell proliferation and survival, Crit. Rev. Biochem. Mol. Biol. 48 (2013) 20–38, https://doi.org/10.3109/10409238.2012.735643.
[22] Y. Dong, V.W. Yong, Oxidized phospholipids as novel mediators of neurodegeneration, Trends Neurosci. 45 (2022) 419–429, https://doi.org/10.1016/j.tins.2022.03.002.
[23] R. Volinsky, L. Cwiklik, P. Jurkiewicz, M. Hof, P. Jungwirth, P.K. Kinnunen, Oxidized phosphatidylcholines facilitate phospholipid flip-flop in liposomes, Biophys. J. 101 (2011) 1376–1384, https://doi.org/10.1016/j.bpj.2011.07.051.
[24] Y. Tian, Y. Liu, C. Xue, J. Wang, Y. Wang, J. Xu, Z. Li, Exogenous natural EPA-enriched phosphatidylcholine and phosphatidylethanolamine ameliorate lipid accumulation and insulin resistance via activation of PPARalpha/gamma in mice, Food Funct. 11 (2020) 8248–8258, https://doi.org/10.1039/d0fo01219j.
[25] M.O. Abdullah, R.X. Zeng, C.L. Margerum, D. Papadopoli, C. Monnin, K.B. Punter, C. Chu, M. Al-Rofaidi, N.F. Al-Tannak, D. Berardi, Z. Rattray, N.J.W. Rattray, S. A. Abraham, E.L. Eskelinen, D.G. Watson, D. Avizonis, I. Topisirovic, E.Y.W. Chan, Mitochondrial hyperfusion via metabolic sensing of regulatory amino acids, Cell Rep. 40 (2022) 111198, https://doi.org/10.1016/j.celrep.2022.111198.
[26] P. Tessari, M. Vettore, R. Millioni, L. Puricelli, R. Orlando, Effect of liver cirrhosis on phenylalanine and tyrosine metabolism, Curr. Opin. Clin. Nutr. Metab. Care 13 (2010) 81–86, https://doi.org/10.1097/MCO.0b013e32833383af.
[27] H. Lemos, L. Huang, G.C. Prendergast, A.L. Mellor, Immune control by amino acid catabolism during tumorigenesis and therapy, Nat. Rev. Cancer 19 (2019) 162–175, https://doi.org/10.1038/s41568-019-0106-z.
[28] S.M. Morris Jr., Regulation of enzymes of the urea cycle and arginine metabolism, Annu. Rev. Nutr. 22 (2002) 87–105, https://doi.org/10.1146/annurev.nutr.22.110801.140547.
[29] R.W. Caldwell, P.C. Rodriguez, H.A. Toque, S.P. Narayanan, R.B. Caldwell, Arginase: a multifaceted enzyme important in health and disease, Physiol. Rev. 98 (2018) 641–665, https://doi.org/10.1152/physrev.00037.2016.
[30] C.E. Turner, W.D. Byblow, N. Gant, Creatine supplementation enhances corticomotor excitability and cognitive performance during oxygen deprivation, J. Neurosci. 35 (2015) 1773–1780, https://doi.org/10.1523/JNEUROSCI.3113-14.2015.
[31] T. Sonnweber, A. Pizzini, M. Nairz, G. Weiss, I. Tancevski, Arachidonic acid metabolites in cardiovascular and metabolic diseases, Int. J. Mol. Sci. 19 (2018), https://doi.org/10.3390/ijms19113285.
[32] K. Kabashima, T. Murata, H. Tanaka, T. Matsuoka, D. Sakata, N. Yoshida, K. Katagiri, T. Kinashi, T. Tanaka, M. Miyasaka, H. Nagai, F. Ushikubi, S. Narumiya, Thromboxane A2 modulates interaction of dendritic cells and T cells and regulates acquired immunity, Nat. Immunol. 4 (2003) 694–701, https://doi.org/10.1038/ni943.
[33] G. Arango Duque, A. Descoteaux, Macrophage cytokines: involvement in immunity and infectious diseases, Front. Immunol. 5 (2014) 491, https://doi.org/10.3389/fimmu.2014.00491.
[34] F. Yang, Y. Zhang, H. Ren, J. Wang, L. Shang, Y. Liu, W. Zhu, X. Shi, Ischemia reperfusion injury promotes recurrence of hepatocellular carcinoma in fatty liver via ALOX12-12HETE-GPR31 signaling axis, J. Exp. Clin. Cancer Res. 38 (2019) 489, https://doi.org/10.1186/s13046-019-1480-9.